

## INFLUENCE OF THE SPOOL VELOCITY ON THE PERFORMANCE OF A DIRECTIONAL HYDRAULIC VALVE

Antonio Posa<sup>1</sup>, Paolo Oresta<sup>2</sup> and Antonio Lippolis<sup>2</sup>

<sup>1</sup>The George Washington University - Department of Mechanical and Aerospace Engineering, 801 22nd Street, N.W., Washington, DC 20052, USA

<sup>2</sup>Dipartimento di Meccanica, Matematica e Management, Politecnico di Bari, Viale Japigia 182, 70126, Bari, ITALY

aposa@gwu.edu, p.oresta@poliba.it, lippolis@poliba.it

---

### Abstract

In this paper an accurate numerical method has been used to verify the influence of the spool velocity on the performance of a directional hydraulic valve (4/3, closed center): the flow during the opening phase of the valve has been solved by Direct Numerical Simulation (DNS), using an Immersed-Boundary (IB) technique.

The present results have been compared with the ones of a previous study, based on the same numerical method, but with a stationary spool. The numerical comparisons prove that the "quasi-stationary" hypothesis is approximately correct for present commercial devices, but it is not suitable for future high-speed valves. However it is shown that, even inside the range of the spool velocities currently adopted, for small pressure drops  $\Delta p$  and small openings  $s$  more significant differences arise on the axial forces.

**Keywords:** Direct Numerical Simulation, Directional hydraulic valves, Finite-difference methods, Immersed-Boundary methods

---

### 1 Introduction

The design of the hydraulic valves requires a careful analysis of the flow conditions produced in these devices and an accurate estimate of the global parameters describing their performance. Originally the approach has been experimental. One of the main works is due to Merrit (1967).

As the experimental tests imply significant costs and the strongly unsteady nature of the flow makes it problematic to carry out measurements, during the last few years several numerical studies have been developed, thanks to the enhancements of both the computational resources and the numerical methods (Amirante et al., 2006; Amirante et al., 2007; Bottazzi et al., 2010; Franzoni et al., 2007). These studies, using a RANS (Reynolds Averaged Navier-Stokes) formulation of the Navier-Stokes equations, allowed improving the knowledge of the complex phenomena occurring through the hydraulic valves.

The main purpose of the present work is to provide a comparison between the results with a moving spool and the ones in Posa et al. (2013), where a series of simulations with a stationary spool is analyzed. In both cases the flow problem has been solved by DNS and the fluid-structure interaction has been modelled using an Immersed-Boundary method. No comparison with

experiments was possible because, to the knowledge of the authors, no experimental data are available for the non-stationary case: actually the aim of this work is also to provide a reference for future experimental studies.

Then this paper aims to assess the accuracy of the "quasi-stationary" hypothesis, on which the numerical studies on the hydraulic valves have been usually based (Borghi et al., 2000; Del Vescovo and Lippolis, 2003; Yang, 2006). The behavior of the device at each instant is well approximated by its stationary behavior with the same boundary conditions of that instant. This assumption implies for a directional valve that it is possible to simulate its working conditions at each opening without taking into account the motion of its spool.

In the past one of the authors of this paper published a similar study (Del Vescovo and Lippolis, 2006), but the flow was solved using a RANS formulation and the "dynamic mesh" technique. This methodology implies the updating of the computational grid at each time step, to fit the new boundary conditions, i.e., the new position of the spool. That work proved that the "quasi-stationary" hypothesis is fairly correct for commercial valves, but some issues in that simulations persuaded the authors to return to this topic: first of all, in the non-stationary simulations the Coanda effect (i.e., the reattachment of the jet from the restricted section on a sidewall of the discharge chamber of the valve) persisted

---

This manuscript was received on 26 January 2013 and was accepted after revision for publication on 17 June 2013

during the valve opening well beyond a reasonable assumption. This result was also inconsistent with the one from the simulations with steady spool.

As shown by Posa et al. (2013), the phenomena in the present flow problem are highly unsteady, above all downstream of the restricted section. Therefore a time-averaged approach, as the RANS formulation, is not well suited for these flows. In fact, in the RANS methods the unsteady physics is taken into account by turbulence models, needing a careful definition of some parameters: this is not trivial, above all for internal flows (Wilcox, 2001). On the other hand in this field a DNS study is feasible: the order of magnitude of the Reynolds numbers for the flows inside the hydraulic valves is  $O(10^3)$ , thanks to the high viscosities of the mineral oils and the limited sizes of the devices. Thus, in the present study the DNS methodology was preferred: every fluid structure is simulated and the instantaneous evolution of the flow field is accurately described.

The previous numerical studies on the hydraulic valves discretized the computational domain by body-fitted grids, which were conformal to the body. On the contrary, in the Immersed-Boundary method the grid is regular (Cartesian or cylindrical) and the boundary conditions at the solid body are enforced at the interface nodes by a discrete source term in the momentum equation. There is no requirement that some nodes of the computational grid are on the surface of the body. These features imply several advantages:

- the generation of the grid is simplified and its computational cost is absolutely negligible;
- the grid cells are regular, without the distortions typical of the body-fitted meshes; therefore the discretization of the Navier-Stokes equations is easier and the accuracy of the solution is improved;
- for moving bodies there is no need to generate a new grid at each time step, since the Immersed-Boundary method does not require that the boundary conditions are enforced at nodes on the body surface; it is only necessary to update the interface points and the values of the forcing terms. About the last remark, it is useful to observe that in the body-fitted approach, at each time step, the solution must be interpolated from the old grid to the new one: this causes an additional computational effort, but also a decreased accuracy. Thus, in the present work the DNS methodology has been coupled with the Immersed-Boundary technique.

This study has been carried out by a computational code originally developed by Verzicco et al. (2000). This code has been validated on several flow problems, through comparisons with experiments and other numerical tools (see Cristallo and Verzicco, 2006; Fadlun et al., 2000; Posa et al., 2011; Verzicco et al., 2004).

## 2 Numerical Method

In the present study the incompressible Navier-Stokes equations have been solved numerically. The continuity and the momentum equations in non-dimensional form are respectively:

$$\nabla \cdot \mathbf{u} = 0 \quad (1)$$

$$\frac{\partial \mathbf{u}}{\partial t} + \nabla \cdot \mathbf{u}\mathbf{u} = -\nabla p + \frac{1}{Re} \nabla^2 \mathbf{u} + \mathbf{f} \quad (2)$$

where  $\mathbf{u}$  is the velocity vector,  $t$  the time variable,  $p$  the pressure,  $\mathbf{f}$  the forcing term due to the immersed-boundary and  $Re = UL/\nu$  the Reynolds number; this has been evaluated using a reference velocity  $U$  (the ratio between the flow rate and the cylindrical area of the restricted section), a reference length  $L$  (the axial dimension  $s$  of the restricted section, that is the opening of the valve) and the kinematic viscosity of the fluid  $\nu$ .

In this work the valve opening range is from 0 to 2.0 [mm] and the oil kinematic viscosity has been set equal to 50 [cSt]: on the basis of the simulated pressure drops, given in Sec. 4, the maximum Reynolds number is approximately equal to 3000.

The differential equations have been discretized in time by a fractional-step method (Kim and Moin, 1985; Rai and Moin, 1991), according to the numerical technique discussed by Verzicco and Orlandi (1996): an implicit Crank-Nicolson scheme has been used for the viscous terms, while the convective ones have been treated by an explicit Adams-Bashforth scheme. The accuracy is second order in time. Second-order central finite-differences on a staggered grid have been used for the spatial derivatives. This approximation improves the accuracy of the solution, avoiding numerical dissipation.

The adopted value of the Courant-Friedrichs-Lewy (CFL) number has been based on the stability requirements for the discretization in time of the convective terms of the momentum equation, since the viscous ones have been treated implicitly: the theoretical stability limit for the second order Adams-Bashforth scheme is  $CFL = 1$ , but for the present study a conservative value of 0.5 has been selected. The average time step was in the range from  $5.6 \times 10^{-8}$  [s] for the maximum  $\Delta p$  to  $1.8 \times 10^{-7}$  [s] for the minimum  $\Delta p$ .

## 3 The Immersed-boundary Method

In the IB method the body is “immersed” into a regular grid, Cartesian or cylindrical: in general, no computational node is on the surface of the solid boundary, since the grid is not conformal to the body.

The computational nodes are marked as interior (inside the immersed-boundary), exterior (in the fluid domain) and interface points: in the present formulation they are the ones in the fluid domain having at least one adjacent interior node. The no-slip boundary conditions on the surface of the immersed body are enforced at the interface points by means of the force  $\mathbf{f}$  in the momentum equation (Eq. 2). As in Mohd-Yusof (1997), this forcing term has been evaluated according to Eq. 3, using the direct forcing approach.

$$\mathbf{f}^{l+1/2} = \frac{V_i - \mathbf{u}^l}{\Delta t} - RHS^{l+1/2} \quad (3)$$

In Eq. 3  $\mathbf{u}^l$  is the velocity at the last time level,  $V_i$  the velocity boundary condition at the interface points and  $RHS^{l+1/2}$  takes into account the viscous, convective

and pressure gradient terms in the discretized form of Eq. 2 at the intermediate time level of the fractional-step method.

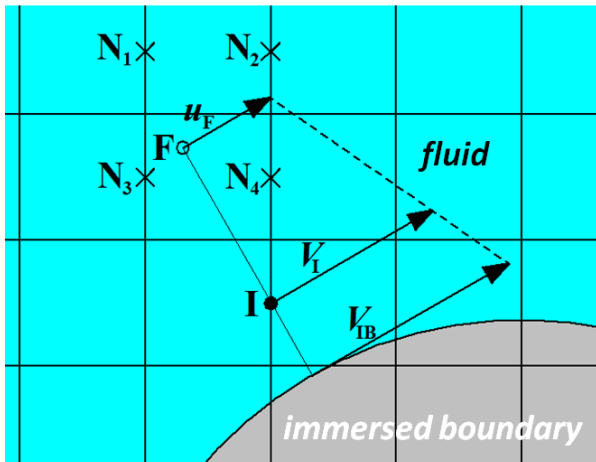


**Fig. 1:** Definition of the boundary condition  $V_I$  at the interface node  $I$ : linear interpolation along the direction normal to the body between the fluid point  $F$  and the surface of the immersed boundary. The grid nodes  $N_1, N_2, N_3, N_4$  are considered to estimate the velocity at the point  $F$

A linear interpolation between the surface of the immersed-boundary and a fluid point  $F$  has been used to evaluate the boundary condition at any interface node  $I$ , as shown in Fig. 1, where  $u_F$  and  $V_{IB}$  are respectively the velocities at  $F$  and on the body. As suggested by Balaras (2004), the point  $F$  has been chosen along the outward normal direction to the immersed-boundary, one grid cell from the interface node  $I$ . The regular grid, which does not conform to the surface of the body, implies that in general  $F$  is not a grid node; therefore the velocity  $u_F$  has been found in the two-dimensional domain by a bilinear interpolation, involving the neighboring nodes of the computational grid ( $N_1, N_2, N_3, N_4$  in Fig. 1).

In the case of moving bodies, as the one treated here, the immersed-boundary method requires that the interface nodes and their positions relative to the body must be updated at each time step. This did not cause any issue of instability or inaccuracy in the near wall flow when the surface of the moving spool crossed a node of the computational grid during the simulations discussed here. In fact, the velocities in the fluid domain are much higher (more than 1 order of magnitude) than the ones of the spool. Since the time step is defined by the CFL condition, the passage of the moving spool across a computational cell is a smooth process, requiring at least about 100 time steps.

More details on the IB methods are provided in Iaccarino and Verzicco (2003) and in Mittal and Iaccarino (2005). Recent studies carried out by means of this technique and involving moving boundaries can be found in de Tullio et al. (2012), Posa et al. (2011) and Vanella et al. (2010).

## 4 Computational Set Up

The simulations have been performed on a two-dimensional domain with conditions of axial symmetry, considering a meridian section of the valve. In fact, except for the adduction and discharge connections, the geometry of the valve is axisymmetric. Then the circumferential flows, due to the lack of symmetry of the inflow and the outflow channels, have been neglected.

The simulated geometry is plotted in Fig. 2: the positions of the inflow and outflow sections are shown and the dimensions of the valve are provided. In this figure  $s$  represents the opening, which is the axial dimension of the restricted section, defined by the spool and valve body edges. More details about the geometry can be found in Posa et al. (2013).

Dirichlet boundary conditions have been enforced at the inflow and convective boundary conditions at the outflow, along the radial direction.

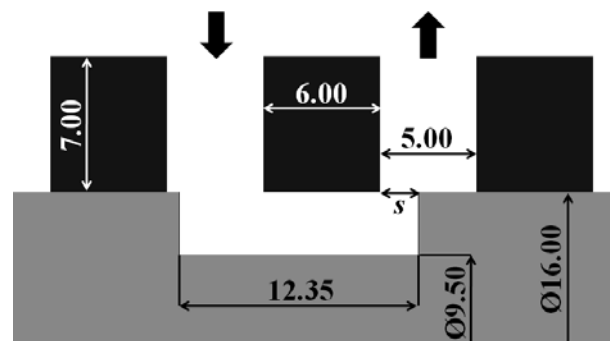


**Fig. 2:** Detail of the meridian section of the valve. Its dimensions are in [mm]. The valve body is represented in black, the spool in gray

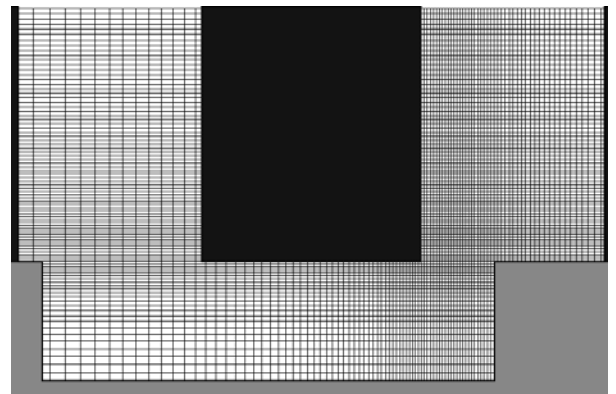


**Fig. 3:** Computational grid. For clarity only 1 point every 4 is shown

The computational grid used for this study is the same considered in Posa et al. (2013): it is composed of  $N_r = 359$  nodes along the radial (vertical) direction and  $N_z = 419$  nodes along the axial (horizontal) one. As discussed in Posa et al. (2013), the results on a finer grid proved the accuracy of the simulations based on the present discretization of the computational domain. In Fig. 3 a simplified representation of the grid is shown (only 1 point every 4 is plotted): it is finer on the restricted section and downstream, in the discharge chamber. In fact, those areas of the computational domain are characterized by a more complex physics. The

minimum grid step, on the restricted section, is equal to 0.02 [mm]. The results of the simulations verified that the resolution adopted at the restricted section is suitable for the present flow problem: at the smallest analyzed opening (0.1 [mm]) the maximum turbulent Reynolds number is lower than 7 and entails a Kolmogorov length scale approximately equal to 0.024 [mm].

In Fig. 4 the representation of a detail of the computational grid in Fig. 3 highlights also that close to the edges the definition of the outward normal direction (arrows) at the interface nodes (filled circles, having neighboring interior nodes along the grid directions) does not generate ambiguities. The hollow circle in the same figure, close to the edge, is not an interface node. It has no adjacent interior nodes along the grid lines; therefore the momentum equations do not involve points inside the immersed-boundary.

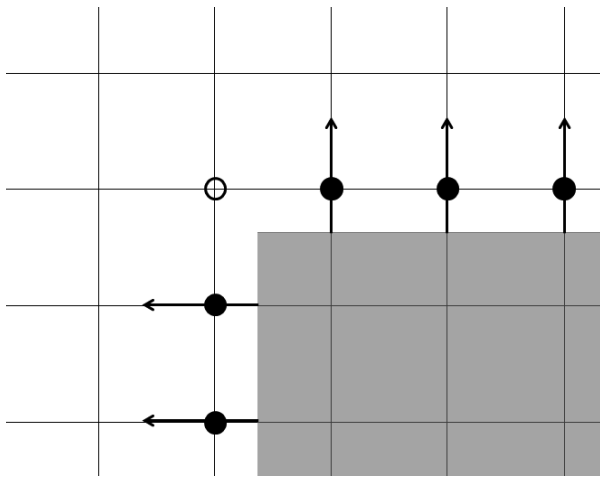


**Fig. 4:** Detail of Fig. 3 near the right edge of the spool. Filled circles represent interface nodes and arrows the local outward normal directions. The hollow circle is a fluid point, having no adjacent interior nodes along the grid lines.

Two different velocities of the spool  $v_s$  have been analyzed: the first, equal to 0.1 [m/s], is in the current range of the commercial directional valves, the second, equal to 1.0 [m/s], will be realistic for future high-speed valves. The spool velocity has been assumed constant, starting from the minimum simulated opening (0.1 [mm]). The spool accelerations have not been considered, but this was supposed of minor importance in the fluid dynamics perspective, since the disagreement between the simulations with stationary and moving spool is due to the different development of the boundary layer, which is related mainly to the spool velocity.

For each value of  $v_s$  four different pressure drops have been simulated, approximately equal to 60, 30, 15 and 7.5 [bar]. It must be noted that the present numerical code requires a Dirichlet boundary condition for the inflow velocity, which means that the flow rate must be set; however, since it has been considered more useful to develop a study with a roughly constant pressure drop, an iterative procedure has been carried out. Initially a flow rate linearly dependent on the spool position has been imposed. Then, based on the pressure drop provided by the simulations, the flow rate has been corrected; for this correction  $\Delta p$  has been assumed

proportional to the square of the flow rate, which is statistically correct. This procedure has been iterated until convergence to the chosen pressure drop with adequate precision.

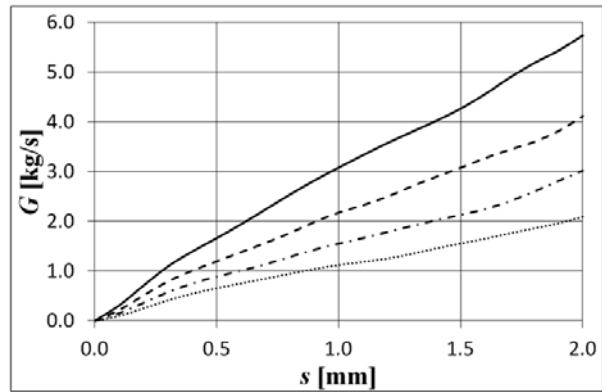


**Fig. 5:** Mass flow as a function of the valve opening with  $v_s=0.1$  [m/s]. Solid line:  $\Delta p=100\% \Delta p_{max}$ ; dashed line  $\Delta p=50\% \Delta p_{max}$ ; dash-dotted line  $\Delta p=25\% \Delta p_{max}$ ; dotted line:  $\Delta p=12.5\% \Delta p_{max}$

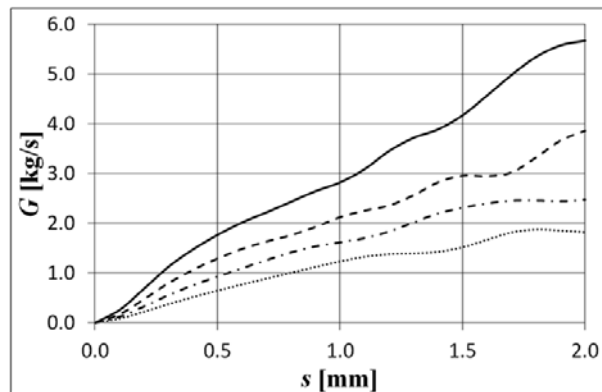


**Fig. 6:** Mass flow as a function of the valve opening with  $v_s=1.0$  [m/s]. Solid line:  $\Delta p=100\% \Delta p_{max}$ ; dashed line  $\Delta p=50\% \Delta p_{max}$ ; dash-dotted line  $\Delta p=25\% \Delta p_{max}$ ; dotted line:  $\Delta p=12.5\% \Delta p_{max}$

The evolution of the mass flow  $G$  as a function of the valve opening  $s$  for each simulated pressure drop is represented in Fig. 5 and 6 respectively for the two spool velocities of 0.1 and 1.0 [m/s]. It is evident that with the lower speed (Fig. 5) the flow rate is roughly a linear function of the valve opening. In the second case (Fig. 6) the linearity is lost.

A parallel OpenMP code has been used to carry out the simulations: each test has been performed on 4 processors. The computational times are reported in Table 1: the evolution of the CPU time is nearly proportional to the flow rate, as the simulations have been done with a constant CFL. Furthermore,  $\Delta t$  is not significantly affected by the spool speed, since  $v_s$  does not influence substantially the maximum velocity in the flow field; thus the computational time necessary to simulate the period of motion of the spool during the valve opening is about proportional to  $1/v_s$ .

**Table 1:** Computational times of the simulations with moving spool.

$\Delta p/\Delta p_{\max}$	CPU time ( $v_s = 0.1$ [m/s])	CPU time ( $v_s = 1.0$ [m/s])
100 %	33[h] 40[min]	3[h] 32[min]
50 %	20[h] 31[min]	2[h] 15[min]
25 %	13[h] 52[min]	1[h] 27[min]
12.5 %	9[h] 33[min]	1[h] 3[min]

## 5 Analysis of the Global Parameters

A comparison between the simulations performed with moving spool and the ones with stationary spool is presented here by the analysis of the global parameters. These parameters are crucial to summarize and to understand the performance of a valve. In this section their time-averages are reported every 0.1 [mm] at 20 positions during the motion of the spool. For each location the instantaneous values have been averaged in the symmetric range of 0.1 [mm] centered at that position.

The discharge coefficient  $C_e$  is defined as the ratio between the actual flow rate and the theoretical one, as in Eq. 4.

$$C_e = \frac{Q}{\pi D s \sqrt{\frac{2\Delta p}{\rho}}} \quad (4)$$

In Eq. 4  $Q$  is the volumetric flow rate,  $D$  the external diameter of the spool and  $\rho$  the density of the working fluid, while the other quantities have been already defined above. The theoretical flow rate is given by the area of the restricted section and the velocity of the fluid on the same section, based on the Borda hypothesis: the flow is assumed isentropic upstream the restricted section and isobaric downstream.

The force parameter  $K$  is the non-dimensional axial force on the spool. It is defined as in Eq. 5:

$$K = \frac{F}{\pi \frac{D^2 - d^2}{4} \Delta p} \quad (5)$$

where  $F$  is the dimensional axial force and  $d$  the internal diameter of the spool.

### 5.1 Discharge Coefficient and Angle

Figure 7 shows the dependence of the discharge coefficient on  $s$  for the maximum and the minimum pressure drops and a spool speed equal to 0.1 [m/s]. In the same figure the results of the simulations with steady spool are also represented: the "quasi-stationary" assumption is fairly correct in this case.

In Fig. 7 the maximum of the discharge coefficient can be justified considering that for very small values of  $s$  the viscous effects on the discharge coefficient are significant, but during the opening their influence de-

creases, because of the increasing area of the restricted section. The boundary layer thickness depends on the flow velocity and is almost not affected by the valve opening; therefore the percentage reduction of the flow rate, caused by the presence of the boundary layer, decreases during the valve opening. This explains the growth of the discharge coefficient during the early stages of the opening period, but larger values of  $s$  are also responsible for reduced values of the discharge angle  $\vartheta_2$  (the mean angle between the spool axis and the jet on the restricted section), as shown in Fig. 8: this causes a decreased section of vena contracta and thus a reduced discharge coefficient.

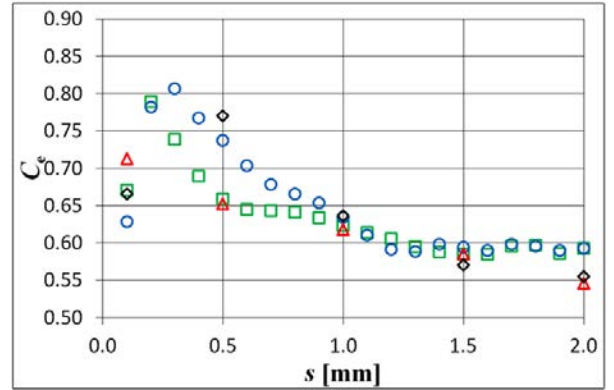


**Fig. 7:** Discharge coefficient  $C_e$  as a function of the valve opening for  $v_s = 0.1$  [m/s]. Maximum pressure drop ( $\Delta p = 100\% \Delta p_{\max}$ ): with stationary spool (red triangles); with moving spool (green squares). Minimum pressure drop ( $\Delta p = 12.5\% \Delta p_{\max}$ ): with stationary spool (black diamonds); with moving spool (blue circles)

In Fig. 7 it is also interesting to see that for the smallest simulated pressure drop the maximum of  $C_e$  occurs for higher values of  $s$ , in comparison with the case of the largest  $\Delta p$ . This result is due to the stronger influence of viscosity on the restricted section for smaller pressure drops and flow rates and also to the Coanda effect, which produces a higher value of the discharge angle: the reattachment of the jet at small openings has been observed for every simulated  $\Delta p$ , but it is more visible for decreased pressure drops.

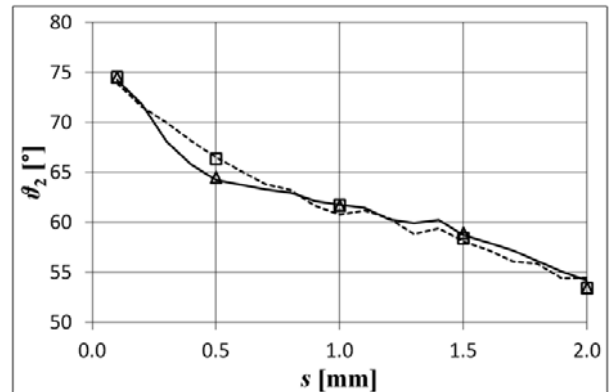


**Fig. 8:** Discharge angle  $\vartheta_2$  as a function of the valve opening for  $v_s = 0.1$  [m/s]. Triangles and solid line:  $\Delta p = 100\% \Delta p_{\max}$ ; squares and dashed line:  $\Delta p = 12.5\% \Delta p_{\max}$ . Stationary spool: symbols; moving spool: lines

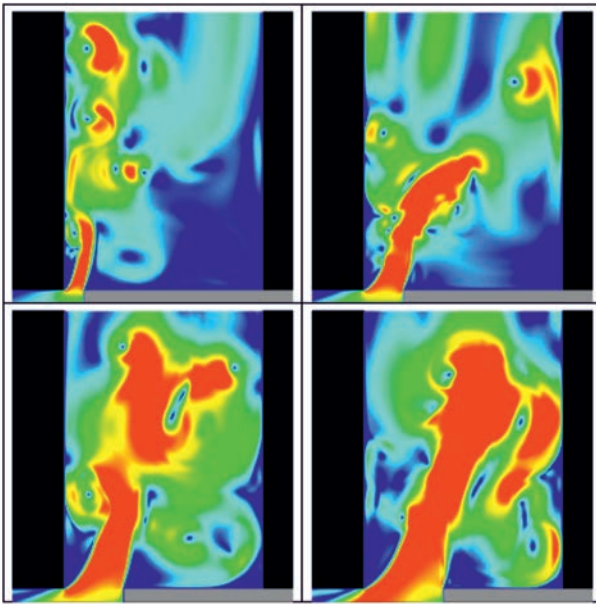


**Fig. 9:** Evolution of the instantaneous velocity fields in the discharge chamber during the opening of the valve for  $v_s = 0.1$  [m/s] and  $\Delta p = 100\% \Delta p_{max}$ . The velocity scale ranges from 0 (blue) to 110 (red) [m/s]

Figure 8 confirms that for commercial values of spool velocity ( $v_s = 0.1$  [m/s]) the quasi-stationary hypothesis is quite accurate. Moreover the non-stationary simulations verified that for very small and large valve openings the discharge angle is roughly not dependent on the pressure drop, as shown by the computations with steady spool in Posa et al. (2013). Some differences have been found only for values of  $s$  around 0.5 [mm]: because of the Coanda effect, lower pressure drops produce larger values of  $\vartheta_2$ .

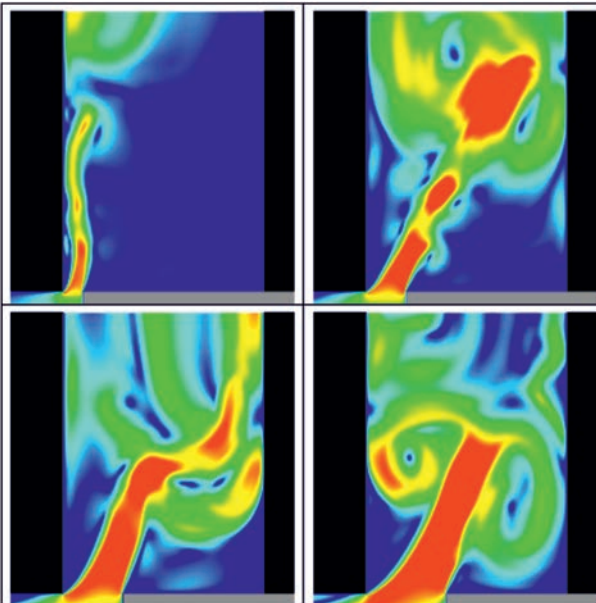


**Fig. 10:** Evolution of the instantaneous velocity fields in the discharge chamber during the opening of the valve for  $v_s = 0.1$  [m/s] and  $\Delta p = 12.5\% \Delta p_{max}$ . The velocity scale ranges from 0 (blue) to 40 (red) [m/s]

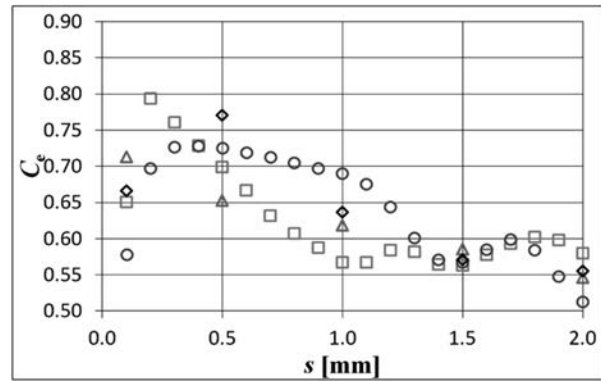


**Fig. 11:** Discharge coefficient  $C_e$  as a function of the valve opening for  $v_s = 1.0$  [m/s]. Maximum pressure drop ( $\Delta p = 100\% \Delta p_{max}$ ): with stationary spool (red triangles); with moving spool (green squares). Minimum pressure drop ( $\Delta p = 12.5\% \Delta p_{max}$ ): with stationary spool (black diamonds); with moving spool (blue circles)

In Fig. 11 the same information of Fig. 7 is given, but for  $v_s = 1.0$  [m/s]: in this case the influence of the unsteady effects associated with the motion of the spool is considerable. In particular, it is interesting to see that for the smallest pressure drop the area of higher discharge coefficients on the right of the peak is enlarged in comparison with the results with stationary spool and with  $v_s = 0.1$  [m/s]. This is verified also for the highest  $\Delta p$ , but in the latter case that behavior of  $C_e$  involves a smaller range of openings. This result is due to a different development of the Coanda effect while the spool is moving. For higher spool speeds the reattachment of the jet, downstream of the restricted section, affects a longer part of the valve opening period and less vortices develop inside the discharge chamber: this increases the value of the angle  $\vartheta_2$  and the discharge coefficient.

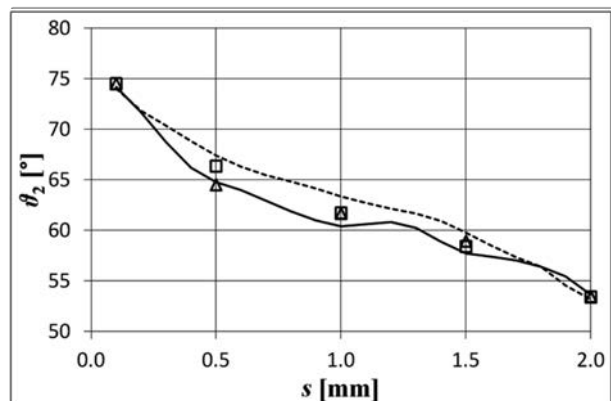


**Fig. 12:** Discharge angle  $\vartheta_2$  as a function of the valve opening for  $v_s = 1.0$  [m/s]. Triangles and solid line:  $\Delta p = 100\% \Delta p_{max}$ ; squares and dashed line:  $\Delta p = 12.5\% \Delta p_{max}$ . Stationary spool: symbols; moving spool: lines

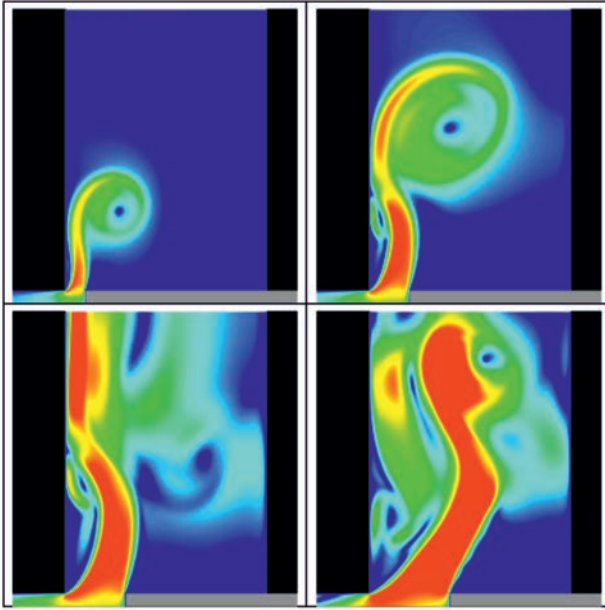


**Fig. 13:** Evolution of the instantaneous velocity fields in the discharge chamber during the opening of the valve for  $v_s = 1.0$  [m/s] and  $\Delta p = 12.5\% \Delta p_{max}$ . The velocity scale ranges from 0 (blue) to 40 (red) [m/s]

The influence of the increased velocity of the spool on the discharge angle is represented in Fig. 12. For the smallest pressure drop at the mean openings the values of  $\vartheta_2$  are larger when the motion of the spool is taken into account during the simulation, since in that case the Coanda effect disappears completely only at the end of the opening phase. On the contrary, for the largest pressure drop the detachment of the jet from the left wall of the discharge chamber is faster: this improves the agreement with the results provided by the simulations with stationary spool.

In order to prove the above remarks for Fig. 11 and 12, in Fig. 13 some instantaneous velocity fields are represented from the simulation with  $v_s = 1.0$  [m/s] and minimum pressure drop: they refer to the same openings considered above for Fig. 9 and 10. Fig. 13 shows that a faster opening phase of the valve produces a relatively longer reattachment of the jet on the left wall of the discharge chamber during the motion of the spool.

## 5.2 Flow Forces

The reliability of the quasi-stationary hypothesis for commercial valves has been verified also by the trend of the axial force on the spool during its motion, not reported here. However more significant percentage differences occur for small openings and pressure drops. This is more evident for large values of  $v_s$ , as pointed out in Fig. 14, where those results are plotted as a function of the valve opening for each simulated pressure drop, with  $v_s = 1.0$  [m/s]. Those differences are provided as percentages of the forces evaluated considering the moving spool, as in Eq. 6, where the superscripts  $m$  and  $s$  refer respectively to the simulations with moving and stationary spool.

$$\Delta F = 100 \frac{F^m - F^s}{F^m} \quad (6)$$

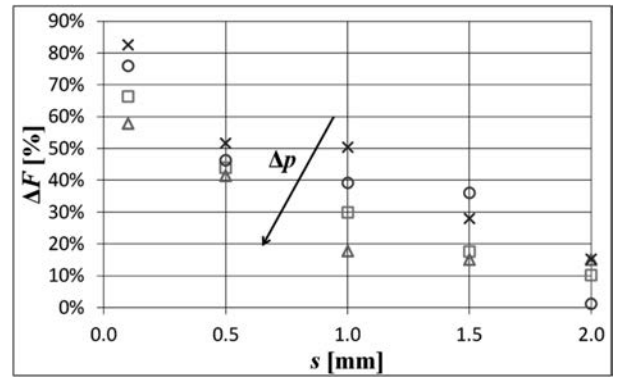


**Fig. 14:** Percentage differences between the axial forces on the spool from the simulations with moving and stationary spool: dependence on the valve opening for  $v_s = 1.0$  [m/s] and different pressure drops. Red triangles:  $\Delta p = 100\% \Delta p_{max}$ ; green squares:  $\Delta p = 50\% \Delta p_{max}$ ; blue circles:  $\Delta p = 25\% \Delta p_{max}$ ; violet times:  $\Delta p = 12.5\% \Delta p_{max}$

In Fig. 14 the values of  $\Delta F$  increase with decreasing  $\Delta p$ ; this result is consistent with the one reported in Del Vescovo and Lippolis (2006). The present analysis highlights also that  $\Delta F$  is larger at the smaller openings, as shown in Fig. 14 for each pressure drop. This trend has been verified also in the range of the commercial valves (spool velocity of 0.1 [m/s]), but in that case the error due to the quasi-stationary hypothesis is less substantial: for the smallest simulated  $\Delta p$  and  $s = 0.1$  [mm],  $\Delta F$  was roughly equal to 25 % with  $v_s = 0.1$  [m/s], while it was larger than 80 % with  $v_s = 1.0$  [m/s].

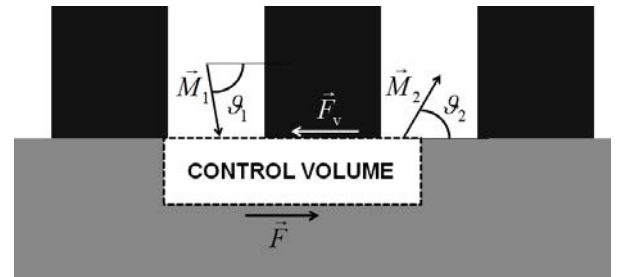


**Fig. 15:** Control volume considered in Eq. 7

As proved in Del Vescovo and Lippolis (2006), using the momentum equation on the control volume of Fig. 15,  $F$  can be expressed as in Eq. 7.

$$F = F_v + M_{2ax} - M_{1ax} + \rho L_1 \dot{Q} \quad (7)$$

In Eq. 7  $F_v$  is the valve body viscous force,  $M_{1ax}$  and  $M_{2ax}$  are the axial components of the momentum flows on the inflow and on the outflow sections of the control volume and  $\rho L_1 \dot{Q}$  is the main term of the inertial component of the axial force on the spool, where  $L_1$  is the mean axial length of the stream tubes and  $\dot{Q}$  the time derivative of the volumetric flow rate.

Considering Eq. 7  $\Delta F$  can be written as in Eq. 8.

$$\Delta F = \Delta F_v + \Delta F_M + \Delta F_i \quad (8)$$

In Eq. 8  $\Delta F_v$ ,  $\Delta F_M$  and  $\Delta F_i$  are respectively:

$$\Delta F_v = 100 \frac{F_v^m - F_v^s}{F^m} \quad (9)$$

$$\Delta F_M = 100 \frac{(M_{2ax} - M_{1ax})^m - (M_{2ax} - M_{1ax})^s}{F^m} \quad (10)$$

$$\Delta F_i = 100 \frac{\rho L_1 \dot{Q}}{F^m} \quad (11)$$

Fig. 16 represents the components of  $\Delta F$  for the smallest simulated pressure drop and  $v_s = 1.0$  [m/s]: the main term is the inertial one  $\Delta F_i$ , whereas the one due to the momentum flows  $\Delta F_M$  is much less important; the viscous component is absolutely negligible.

For clarity, only the case with the minimum pressure drop has been reported here, but also the other tests lead to the same conclusions, although the values are decreased.

The result above suggests that, if the evolution of the flow rate through the valve during its opening is approximately known, a good estimate of the flow forces can be provided also by the “stationary” method, even for small openings and pressure drops and for spool speeds much higher than the commercial ones: the inertial term can be evaluated by means of the time derivative of the flow rate, while the error on the other components of the axial force on the spool is negligible. This method has been utilized in the past in some works (Borghi et al., 1998; Krishnaswamy and Li, 2002) and the present study verified that it can be considered correct.

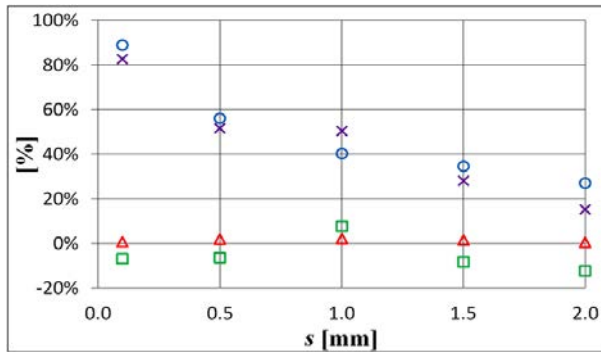


**Fig. 16:** Components of the percentage difference between the axial forces on the spool from the simulations with moving and stationary spool: dependence on the valve opening for the smallest simulated pressure drop ( $\Delta p = 12.5\% \Delta p_{max}$ ) and  $v_s = 1.0$  [m/s]. Red triangles:  $\Delta F_v$ ; green squares:  $\Delta F_M$ ; blue circles:  $\Delta F_i$ ; violet times:  $\Delta F$

The behavior of the axial force on the moving spool, described in Fig. 14 and 16, can be justified on the basis of the momentum equation. In fact Eq. 7 can be written as in Eq. 12 (more details are given in Del Vescovo and Lippolis (2006)):

$$F = F_v + 2\Delta p C_e^2 \left( \frac{A_2}{\tan \vartheta_2} - \frac{A_2^2}{A_1 \tan \vartheta_1} \right) + \rho L_1 \sqrt{\frac{2\Delta p}{\rho}} \left( A_2 \frac{dC_e}{dt} + \frac{dA_2}{dt} C_e \right) \quad (12)$$

In Eq. 12  $A_1$  and  $A_2$  are the areas of the inflow and the outflow sections of the control volume, whereas  $\vartheta_1$  and  $\vartheta_2$  are the angles between the spool axis and the mean flow velocities on the same sections, as represented in Fig. 15.

Eq. 12 shows that the second term of the right-hand side, tied to the momentum flows, is proportional to the pressure drop, while the third one, that is the inertial term, is dependent on the square root of  $\Delta p$ ; hence for small pressure drops its relative weight in the global force is increased, causing higher values of  $\Delta F$ .

Furthermore Eq. 12 allows noticing that, while the component from the momentum flows is roughly a linear function of the valve opening, this is not the case of the inertial term. In fact, Eq. 12 can be expressed as in Eq. 13, where a radial inflow has been assumed.

$$F = F_v + 2\Delta p C_e^2 \frac{\pi D s}{\tan \vartheta_2} + \rho L_1 \sqrt{\frac{2\Delta p}{\rho}} \pi D \left( s \frac{dC_e}{dt} + v_s C_e \right) \quad (13)$$

According to Eq. 13, the evolution of the discharge coefficient in Fig. 7 and 11 implies a rapid increase of the inertial force for very small openings and roughly constant values for the larger ones. This explains the reduction of  $\Delta F_i$  during the motion of the spool.

Finally in Fig. 17 and 18 the force parameter  $K$  is represented as a function of the valve opening  $s$  for both the analyzed speeds of the spool. As shown in Eq. 13, if the viscous and the inertial components of  $F$  are negligible, the parameter  $K$  is not dependent on  $\Delta p$  and is proportional to  $s$ .

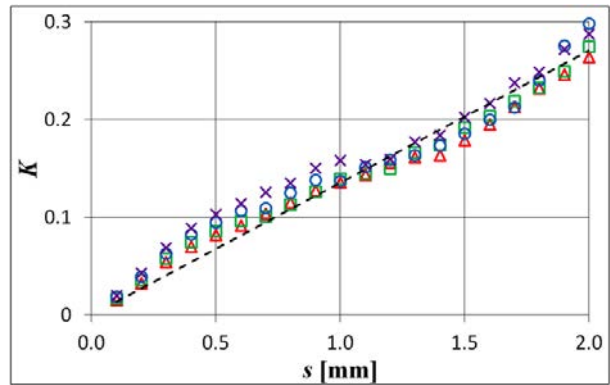


**Fig. 17:** Force parameter  $K$  as a function of the valve opening from the simulations with moving spool for  $v_s = 0.1$  [m/s]. Red triangles:  $\Delta p = 100\% \Delta p_{max}$ ; green squares:  $\Delta p = 50\% \Delta p_{max}$ ; blue circles:  $\Delta p = 25\% \Delta p_{max}$ ; violet times:  $\Delta p = 12.5\% \Delta p_{max}$ . Also the dashed linear regression line is represented

In Fig. 17 the evolution of  $K$  as a function of  $s$  is approximately linear. Actually there are some significant deviations from the linear trend, especially for small openings. This has been observed also for the simulations with stationary spool in Posa et al. (2013) and can be explained considering the Coanda effect: it increases the discharge coefficient; this produces higher values of  $F$  and  $K$ , as proved by Eq. 12.

Since the Coanda effect declines during the motion of the spool,  $C_e$  decreases: this causes also a reduction of the slope of  $K$  as a function of  $s$ . Furthermore, the Coanda effect is stronger for small pressure drops, therefore its influence on the trend of the force parameter is more evident when  $\Delta p = 12.5\% \Delta p_{max}$  than when  $\Delta p = 100\% \Delta p_{max}$ .

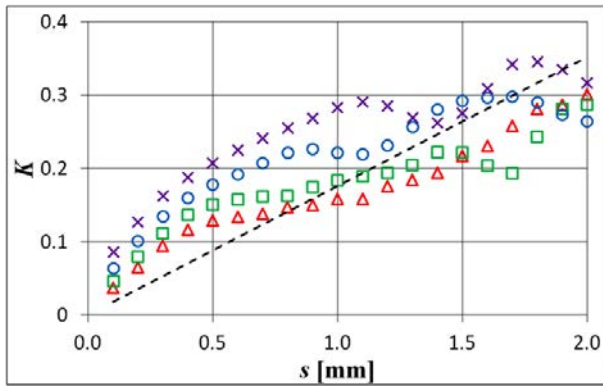


**Fig. 18:** Force parameter  $K$  as a function of the valve opening from the simulations with moving spool for  $v_s = 1.0$  [m/s]. Red triangles:  $\Delta p = 100\% \Delta p_{\max}$ ; green squares:  $\Delta p = 50\% \Delta p_{\max}$ ; blue circles:  $\Delta p = 25\% \Delta p_{\max}$ ; violet times:  $\Delta p = 12.5\% \Delta p_{\max}$ . Also the dashed linear regression line is represented

The results in Fig. 17 confirm the ones from the previous study with stationary spool, but the dependence of  $K$  on  $\Delta p$  is increased. This is due to the inertial force on the spool: its component in  $K$  is inversely proportional to the square root of  $\Delta p$ , thus for the smallest  $\Delta p$  the values of  $K$  are further higher than the ones for larger pressure drops.

As discussed above, a larger value of  $v_s$  is associated with a larger range of valve openings affected by the Coanda effect. Therefore the areas where  $K$  deviates from the linear behavior are enlarged and the force parameter is increased, as proved by the comparison of Fig. 18 with Fig. 17.

## 6 Conclusions

In this paper the flow through a directional hydraulic valve (4/3, closed center) has been analyzed using an unsteady numerical approach, based on the Direct Numerical Simulation, coupled with an Immersed-Boundary technique. A comparison with the study presented in Posa et al. (2013) has been developed. In Posa et al. (2013) the flow has been solved with a stationary spool, considering some specific values of the valve opening, while here the physics has been simulated with a moving spool during the opening phase. Two speeds of the spool have been studied, respectively equal to  $v_s = 0.1$  [m/s] and  $v_s = 1.0$  [m/s]. The former is in the range of the current commercial valves; the latter is realistic for future high-speed devices.

The flow has been simulated in a 2D computational domain with conditions of axial symmetry. The analysis of the flow problem has been carried out by the solution of the instantaneous flow fields and the estimate of the relative statistics: this feature is crucial to get accurate results, due to the strongly unsteady nature of the physics verified by the simulations. The immersed-boundary method allowed avoiding modifications of the computational grid during the motion of the spool. This is beneficial for the simulations performance and the solution accuracy, in comparison with the traditional body-fitted techniques.

Then this study verified if the “quasi-stationary” hypothesis, widely utilized for the simulation of hydraulic devices, is accurate for commercial and future high-speed directional valves.

The comparison of the global parameters, as the discharge coefficient, the discharge angle and the axial force on the spool, proved that the agreement between the two different methods analyzed here is satisfactory for a velocity of the spool of the order of 0.1 [m/s]. On the contrary, the “quasi-stationary” hypothesis cannot be used to simulate high-speed valves.

That comparison showed also that, even in the current range of spool speeds, a simulation with stationary spool does not predict the values of  $F$  with enough accuracy for small openings and pressure drops, because of the inertial term of the flow force, which in those conditions is a significant component of the global force. It has been verified that higher values of  $v_s$  emphasize that issue, which for increased velocities of the spool affects also larger openings and pressure drops. However the analysis of components presented here proved that a good estimate of the axial force can be defined even using the “quasi-stationary” hypothesis, if a correction by the inertial term  $\rho L_1 \dot{Q}$  is introduced, assumed that the time dependence of the flow rate can be approximately determined.

## Nomenclature

$\Delta F$	percentage difference between the axial forces on the moving spool and on the stationary one	[%]
$\Delta F_i$	inertial component of $\Delta F$	[%]
$\Delta F_M$	component of $\Delta F$ associated with the axial momentum flows	[%]
$\Delta F_v$	viscous component of $\Delta F$	[%]
$\Delta p$	pressure drop	[bar]
$\Delta p_{\max}$	maximum pressure drop	[bar]
$\Delta t$	non-dimensional time step	[-]
$\vartheta_1, \vartheta_2$	angles between the axis of the spool and the mean flow velocity respectively on the inflow and the outflow sections of the control volume in Fig. 15	[°]
$\nu$	kinematic viscosity of the working fluid	[cSt]
$\rho$	density of the working fluid	[kg/m <sup>3</sup> ]
$A_1, A_2$	areas of the inflow and the outflow sections of the control volume in Fig. 15	[mm <sup>2</sup> ]
$C_c$	discharge coefficient	[-]
CFL	Courant-Friedrichs-Lewy number	[-]
$D$	external diameter of the spool	[mm]
$d$	internal diameter of the spool	[mm]
$F$	axial force on the spool	[N]
$F_v$	valve body viscous force	[N]
$f$	forcing term in the non-dimensional momentum equation	[-]
$G$	mass flow	[kg/s]
$K$	non-dimensional axial force on the spool	[-]
$L$	characteristic length of the flow problem	[mm]

$L_1$	mean axial length of the stream tubes in the control volume in Fig. 15	[mm]
$l$	index of the last time level	[-]
$M_{1ax}$	axial component of the momentum flow through the inflow section of the control	[N]
$M_{2ax}$	axial component of the momentum flow through the outflow section of the control volume in Fig. 15	[N]
$N_r$	number of grid nodes along the radial direction	[-]
$N_z$	number of grid nodes along the axial direction	[-]
$p$	non-dimensional pressure	[-]
$Q$	volumetric flow rate	[m <sup>3</sup> /s <sup>2</sup> ]
$\dot{Q}$	time derivative of the volumetric flow rate	[m <sup>3</sup> /s <sup>2</sup> ]
$Re$	Reynolds number	[-]
<b>RHS</b>	sum of the discretized viscous, convective and pressure gradient terms of the non-dimensional momentum equation	[-]
$s$	opening of the valve	[mm]
$t$	non-dimensional time	[-]
$U$	characteristic velocity of the flow problem	[m/s]
$u$	non-dimensional velocity vector	[-]
$u_F$	non-dimensional velocity in the fluid domain	[-]
$V_I$	non-dimensional velocity boundary condition at the interface nodes	[-]
$V_{IB}$	non-dimensional velocity on the surface of the immersed-boundary	[-]
$v_s$	spool velocity	[m/s]

## Acknowledgment

The authors are grateful to CASPUR (Consorzio interuniversitario per le Applicazioni di Supercalcolo Per Università e Ricerca) for providing computational resources.

## References

- Amirante, R., Del Vescovo, G. and Lippolis, A.** 2006. Evaluation of the flow forces on an open-centre directional control valve by means of a computational fluid dynamic analysis. *Energy Conversion and Management*, Vol. 47, pp. 1748 - 1760.
- Amirante, R., Moscatelli, P. G. and Catalano L. A.** 2007. Evaluation of the flow forces on a direct (single stage) proportional valve by means of a computational fluid dynamic analysis. *Energy Conversion and Management*, Vol. 48, pp. 942 - 953.
- Balaras, E.** 2004. Modeling complex boundaries using an external force field on fixed Cartesian grids in large-eddy simulations. *Computers & Fluids*, Vol. 33, pp. 375 - 404.
- Borghì, M., Milani, M. and Paoluzzi, R.** 1998. Transient flow forces estimation on the pilot stage of a hydraulic valve. *Proceedings of the 1998 IMECE-ASME International Mechanical Engineering Congress and Exposition - Fluid Power Systems Technology Division*, Anaheim, CA, USA.
- Borghì, M., Milani, M. and Paoluzzi, R.** 2000. Stationary axial flow force analysis on compensated spool valves. *International Journal of Fluid Power*, Vol. 1, pp. 17 - 25.
- Bottazzi, D., Franzoni, F., Milani, M. and Montorsi, L.** 2010. Metering characteristics of a closed center load-sensing proportional control valve. *SAE Paper - International Journal of Commercial Vehicles*, Vol. 2, pp. 66 - 74.
- Cristallo, A. and Verzicco, R.** 2006. Combined Immersed Boundary/Large-Eddy-Simulations of Incompressible Three Dimensional Complex Flow. *Flow Turbulence and Combustion*, Vol. 77, pp. 3 - 26.
- Del Vescovo, G. and Lippolis, A.** 2003. Three-dimensional analysis of flow forces on directional control valves. *International Journal of Fluid Power*, Vol. 4.
- Del Vescovo, G. and Lippolis, A.** 2006. A review analysis of unsteady forces in hydraulic valves. *International Journal of Fluid Power*, Vol. 7, pp. 29 - 39.
- de Tullio, M.D., Nam, J., Pascazio, G., Balaras, E. and Verzicco, R.** 2012. Computational prediction of mechanical hemolysis in aortic valved prostheses. *European Journal of Mechanics - B/Fluids*, Vol. 35, pp. 47 - 53.
- Fadlun, E. A., Verzicco, R., Orlandi, P. and Mohd-Yusof J.** 2000. Combined Immersed-Boundary Finite-Difference Methods for Three-Dimensional Complex Flow Simulations. *Journal of Computational Physics*, Vol. 161, pp. 35 - 60.
- Franzoni, F., Milani, M. and Montorsi, L.** 2007. A CFD multidimensional approach to hydraulic component design. *SAE Transactions - Journal of Commercial Vehicles*, Vol. 116, pp. 246 - 259.
- Iaccarino, G. and Verzicco, R.** 2003. Immersed boundary technique for turbulent flow simulations. *Applied Mechanics Reviews*, Vol. 56, pp. 331 - 347.
- Kim, J. and Moin, P.** 1985. Application of a fractional-step method to incompressible Navier-Stokes equations. *Journal of Computational Physics*, Vol. 59, pp. 308 - 323.
- Krishnaswamy, K. and Li, P. Y.** 2002. On using unstable electrohydraulic valves for control. *Journal of Dynamic Systems, Measurement, and Control*, Vol. 124, pp. 183 - 190.
- Merrit, H. E.** 1967. Hydraulic Control systems. *John Wiley & Sons*, New York.
- Mittal, R. and Iaccarino, G.** 2005. Immersed boundary methods. *Annual Review of Fluid Mechanics*, Vol. 37, pp. 239 - 261.

**Mohd-Yusof, J.** 1997. Combined immersed-boundary/B-spline methods for simulations of flow in complex geometries. *Annual Research Briefs, Center for Turbulence Research*. University of Stanford, pp. 317-327.

**Posa, A., Lippolis, A., Verzicco, R. and Balaras, E.** 2011. Large-eddy simulations in mixed-flow pumps using an immersed-boundary method. *Computers & Fluids*, Vol. 47, pp. 33 - 43.

**Posa, A., Oresta, P. and Lippolis, A.** 2013. Analysis of a directional hydraulic valve by a Direct Numerical Simulation using an immersed-boundary method. *Energy Conversion and Management*, Vol. 65, pp. 497 - 506.

**Rai, M. M. and Moin, P.** 1991. Direct simulations of turbulent flow using finite-difference schemes. *Journal of Computational Physics*, Vol. 96, pp. 15 - 53.

**Vanella, M., Rabenold, P. and Balaras, E.** 2010. A direct-forcing embedded-boundary method with adaptive mesh refinement for fluid-structure interaction problems. *Journal of Computational Physics*, Vol. 229, pp. 6427 - 6449.

**Verzicco, R. and Orlandi, P.** 1996. A finite-difference scheme for three-dimensional incompressible flows in cylindrical coordinates. *Journal of Computational Physics*, Vol. 123, pp. 402 - 414.

**Verzicco, R., Mohd-Yusof, J., Orlandi, P. and Haworth, D.** 2000. Large Eddy Simulation in Complex Geometric Configurations Using Boundary Body Forces. *AIAA Journal*, Vol. 38, pp. 427 - 433.

**Verzicco, R., Fatica, M., Iaccarino, G. and Orlandi, P.** 2004. Flow in an impeller-stirred tank using an immersed-boundary method. *AIChE Journal*, Vol. 50, pp. 1109 - 1118.

**Wilcox, D.** 2001. Turbulence modeling: an overview. *AIAA Paper No. 2001 - 0724*. Washington, DC: American Institute of Aeronautics and Astronautics.

**Yang, R.** 2006. Hydraulic oil flow wall shear effect on valve actuator flow forces. *Proceedings of the 2nd International Conference on Computational Methods in Fluid Power Technology*. Aalborg, DK.



**Antonio Posa**

Born in Bari (Italy) in 1981. B.S. in Industrial Engineering (2004), Politecnico di Bari. M.Sc. in Industrial Engineering (2006), Politecnico di Bari. Faculty Research Assistant (2009), University of Maryland. Ph.D. in Fluid Machinery Engineering (2010), Politecnico di Bari. Faculty Research Assistant (2010-2011), University of Maryland. Post Doctoral Scientist (2012-Present), The George Washington University.



**Paolo Oresta**

Paolo Oresta was born in Taranto on September 8, 1978. He graduated in Mechanical Engineering (2003) and he got the PhD in Environment and Land Engineering (2007) at the Politecnico di Bari. At present he is Assistant Professor at Politecnico di Bari. He investigated the multiphase natural convection (University of Twente, The Netherlands) and the spray tracking (Università del Salento, Italy).



**Antonio Lippolis**

Born in Gioia del Colle (Italy) in 1955. Graduated in Mechanical Engineering (1981) at the Politecnico di Bari. Researcher at the Politecnico di Bari since 1983, at present is Full Professor in Fluid Power Systems. Author and Co-Author of more than 50 papers dealing with Numerical Fluid-Dynamics and Fluid Power.